

# Swarm parameter measurement of hydrogen, considering secondary photonic electron emission

Andreas Hösl

Christian Franck

ETH Zürich, High Voltage Lab

E-mail: [franck@eeh.ee.ethz.ch](mailto:franck@eeh.ee.ethz.ch)

**Abstract.** Discharges in hydrogen at pressures above 1 kPa and a reduced electric field of  $E/N = 100 - 200$  Td show a characteristic current oscillation in Pulsed Townsend experiments. This is explained by secondary emission of electrons from the photo-cathode: some hundreds of nano-seconds after the laser-pulse that released the initial  $10^4 - 10^6$  primary electrons, secondary electrons are emitted from the cathode. Mechanisms discussed in literature are UV-emission from neutral molecules, emission by positive ions reaching the cathode, and back-scattering of excited neutrals. For a measurement up to 500 Td and pressures up to 2 kPa we model different sources, and agree with previous findings that the observed secondary emission is purely due to ultra-violet light below 200 Td: the simulation fits with the complicated form of the oscillating waveform. Obtained swarm parameters agree well with the literature. Our findings suggest a very high efficiency of the photo-cathode for UV light of energies above 8 eV.

## 1. Introduction

The well established Pulsed Townsend method allows the measurement of swarm parameters in a variety of gases: a pulsed UV laser releases electrons from a photo-cathode, which then travel in the applied homogeneous electric field and interact with neutral gas molecules. The displacement current of the charge carriers is measured and evaluated.

The discharge in hydrogen at few kPa pressure and  $E/N = 100 - 200$  Td shows an unusual, oscillating temporal development. A release of electrons some time after the initial laser pulse, and by a different source than the laser, has to be taken into account in order to evaluate the measured waveforms ("secondary emission"). Figure 1 shows an example of such a measurement.

Our motivation for examining hydrogen discharges is mainly the investigation of the photo-cathode. We use hydrogen to "regenerate" the cathode after measuring oxidizing or fluoridating gases, which tend to decrease the efficiency (released electrons per UV photon). After being subjected to a hydrogen discharge at 200 – 400 Td or higher, and

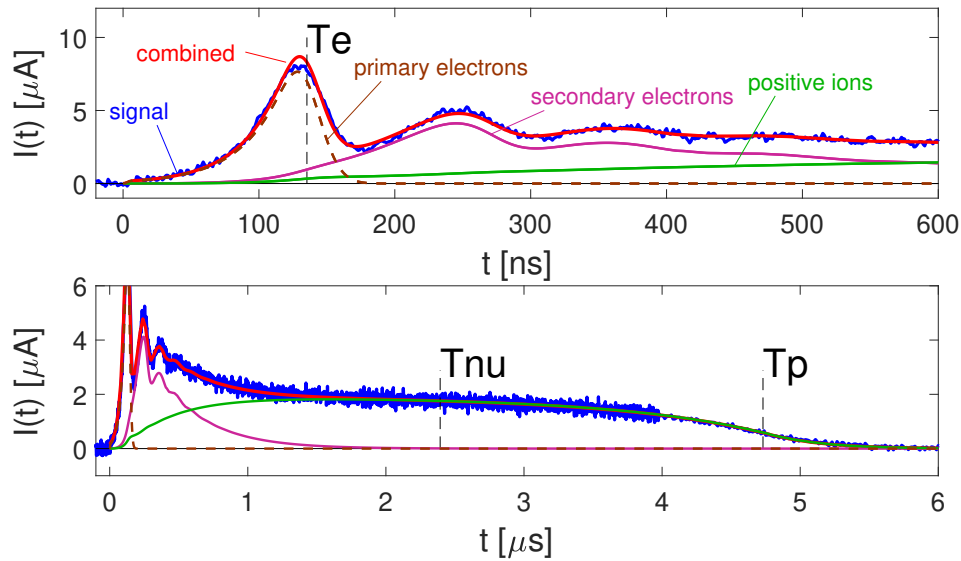


**Figure 1.** A measurement at 130 Td, at a pressure of 1.1 kPa and 25 mm gap distance, on two different time scales. For times before the electron drift time  $T_e = 130$  ns, the typical exponential growth of electrons is observed. Secondary peaks are found at (roughly, but not exactly) multiples of  $T_e$ . The charge contribution of the secondary electrons outweighs the primary electrons by far. The current after  $1 \mu\text{s}$  is then mainly positive ions.

at pressures from 50 – 300 Pa, its efficiency typically increases by a factor of 2 – 10. The reason for this is not entirely clear. Secondly, we aim at modeling secondary emission in order to be able to distinguish between secondary emission and ion detachment effects in other gases, which exhibit large currents at ion-timescales.

The physics of hydrogen can become very complicated at high reduced electric fields above 500 Td; an extensive overview of which is given by Phelps et al [8, 13]. We consider and implement a subset of the variety of discussed cathode phenomena, which are potentially relevant below 500 Td:

- Excitation of the photo-cathode due to positive ions or neutral excited molecules: positive ions neutralize upon arrival at the (photo-)cathode; if the recombination energy is sufficient to remove two electrons (one to neutralize, one to emit) from the cathode material, secondary emission could energetically be possible. The cathode materials are specifically chosen for their low work function, which is usually around 4 – 5 eV, whereas the the ionization energy of hydrogen is 15.4 eV. Phelps [13] gives a different physical explanation and assumes that fast neutral  $H$  atoms (equation 3) are responsible for secondary emission, as observed by Fletcher and Blevin [6] above 220 Td.
- Secondary emission due to UV-photons, for which we consider two variants: First, excitation of neutral molecules upon collision with free electrons, followed by radial emission of a UV photon. Secondly, UV emission upon arrival of an electron at the anode.

Phelps [13] agrees with Blevin and Fletcher [6], that below 300 Td, photo-emission is the dominating process for secondary emission. Our findings further confirm this: modeling UV emission by neutral molecules, proportional to the spatial distribution of electrons, reproduces all waveforms up to 200 Td, and fails above. Phelps and other sources [11, 13] state further that positive ions are the primary source of secondary electron generation above 250 Td. We try a simplified implementation thereof, yet fail to achieve a good overlap of measurement and simulation.

The evaluation of the waveforms is done using a finite volume simulation on GPUs, as is described in [18].

## 2. Kinetic Model

### 2.1. Physical picture

Molecular hydrogen has, compared to other non-noble gases, a comparably high ionization threshold of 15.4 eV:



We model this with a constant rate  $\nu_i$ , and assume that the electron energies are in thermodynamic equilibrium. At high  $E/N$  and low pressures, this introduces a certain error, as soon as ionization time-scales are of the same magnitude as equilibration. The error is difficult to estimate, and was discussed for instance in [15].

The ion clustering

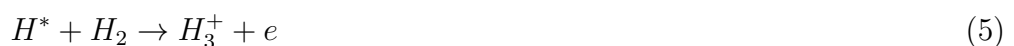


is very efficient [1], and indeed we find ion mobilities that are compatible with reference values for  $H_3^+$ . Dissociative ionization is considered in the complex model of Phelps et al [13], and accounts for a few percent of the total ionization.

For  $H_3^+$  ions of sufficient energy a dissociation into  $H^+$  and  $H_2$  is observed above 250 Td. Phelps states that subsequent charge transfer



would then create fast neutral  $H$  atoms which are capable of releasing electrons from the photo-cathode. Another possible source is subsequent chemo-ionization and associative ionization



with thresholds of 13.7 and 14.7 eV, as considered in [9].

The  $H_2$  dissociative attachment rate



is 2 – 3 orders of magnitudes smaller than the ionization rate over the whole measurement range. The energy required is 7 eV according to Biagi’s cross section set [17] from MAGBOLTZ (version 8.9, source: LXCat [16]), which differs from values of the TRINITY cross section set [14], also on LXCat, which features values around 3.6 eV. Detachment of the electron of  $H^-$  has, for instance, been investigated in [7]. We are unable to observe neither attachment nor detachment in our measurements, as its current contribution is by orders of magnitude lower compared to positive ions and primary electrons. We thus use the results of a Bolsig+ simulation to preset the attachment rate coefficient. Omitting this rate, or introducing detachment, does not visibly change the current shape of our measurements.

The measured total displacement current of the Pulsed Townsend experiment is then given as

$$I_{\text{tot}}(t) = I_e(t) + I_p(t) + I_n(t) = \frac{q_0}{d} \int_0^d \frac{\rho_e(x, t)}{T_e} + \frac{\rho_p(x, t)}{T_p} + \frac{\rho_n(x, t)}{T_n} dx, \quad (7)$$

with elemental charge  $q_0$ , densities  $\rho(x, t)$  of electrons (e), positive ions (p), and negative ions (n), gap drift times  $T_e$ ,  $T_p$  and  $T_n$ . The integral is taken over the gap distance  $d$ .

## 2.2. Fitting method

We use our established method of fitting simulations to measurements, as described in [18]. The finite-volume simulations run on GPUs, to cope with the large computational cost. In the following we describe the additional extensions in order to simulate secondary emission.

## 2.3. Secondary emission modeling

- Model 1, secondary emission due to arriving positive ions/neutral excited atoms at the photo-cathode is modeled straight-forward: at a certain probability, a new electron is released per arriving positive ion.
- Model 2.1, Proportional to the electron density  $\rho_e(x, t)$  at position  $x$ , excited neutral molecules are created. If the life-time of the excitation is below few nano-seconds, the decay of this excitation can be modelled as instantaneously, and is followed by a radial emission of a UV photon (equation (8)).
- Model 2.2, UV light is emitted upon arrival of an electron at the anode, which releases an energy equal to the kinetic energy of the electron plus, possibly, the ”work function” of the anode material. This is implemented similar to model 1.

The equation describing model 2.1 is given as

$$\frac{\partial}{\partial t} \rho_e(x=0, t) = \dots + \nu_{\text{UV}} \int_0^d \rho_e(x, t) g(x) dx. \quad (8)$$

Proportional to the electron density  $\rho_e(x, t)$  at position  $x$ , UV light is emitted and releases electrons from the photo-cathode at  $x = 0$ . Absorption of UV light in the gas is assumed to be negligible.  $g(x)$  is a geometric factor, i.e. probability to hit the photo-cathode for radially emitted light. Our calculation of  $g(x)$  assumes an even distribution of electrons over our cathode of 1.25 cm radius, and neglects transversal diffusion. The geometric factor is maximal at  $x = 0$  at 50 %, and drops to roughly 10 – 20 % at the anode for the measurement gap distances of 1.5 – 3 cm.

### 3. Results

Trying out the different variants of secondary emission, we find that

- Model 1, in which positive ions/neutral atoms release electrons at impact at the cathode does not recreate the measured waveforms. Neither does a combination with UV emission (model 2.1), which we try out for the  $E/N$  range beyond 250 Td.
- Model 2.1, instantaneous UV-emission, explains all waveforms up to 200 Td. Since the temporal evolution of the waveforms as shown in the example plot 1 is relatively complex, we are lead to believe that this is the correct model.
- Model 2.2, in which UV is emitted upon arrival of the electrons of the anode reproduces an oscillations, yet the secondary maxima positions do not fit with the measurement. The model is periodic with the electron drift time, whereas the measured waveforms feature maxima slightly earlier than  $2T_e$ ,  $3T_e$ , ...

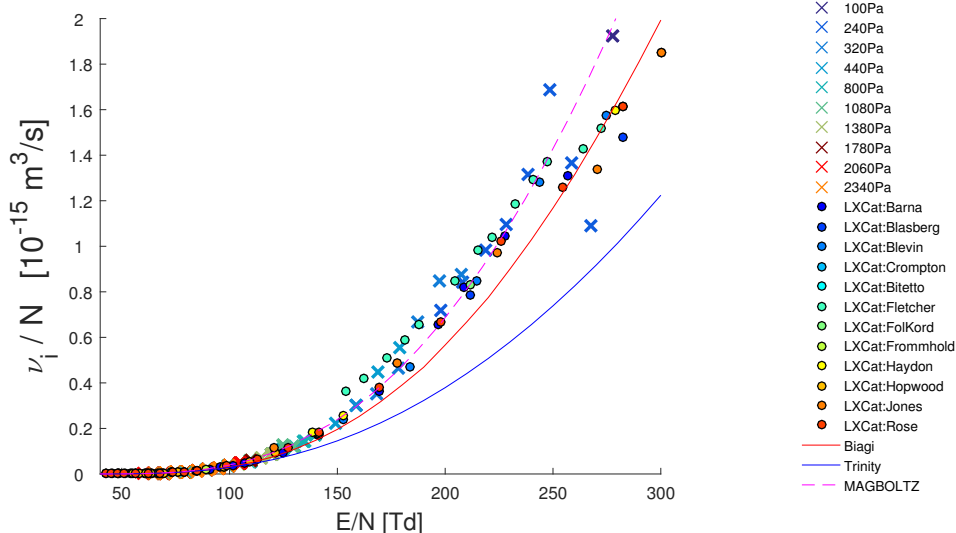


**Figure 2.** The fitted ionization rate coefficient for different measured pressures and  $E/N$ . Our values are compared to literature values from LXCat [16] by different authors, as well as Bolsig+ simulations using the Biagi [17] and Trinity [14] database.

As an output of the fitting process, we obtain the following rate coefficients for model 2.1, assuming instantaneous UV emission of neutral molecules. We compare our findings

to literature results of various authors on LXCat [16], as well as Bolsig+ simulations (2-term Boltzmann approximation) using Biagi's data set (from MAGBOLTZ code version 8.9 [16]) and the TRINITY data set [14]. We further compare to a MAGBOLTZ simulation (Monte-Carlo) with a newer data set, version 11.2 [17].

All references agree with our findings for the ionization rate coefficient below 250 Td, as shown in figure 2. Above, our values show a large spread, while the quality of the fit degrades strongly: currents after the gap crossing time of the positive ion begin to emerge, which cannot be explained within the model. Therefore, our findings at high  $E/N$  are should not be regarded as "fitting results", but should rather illustrate the incipient failure of our model and hint at a different channel of secondary emission.

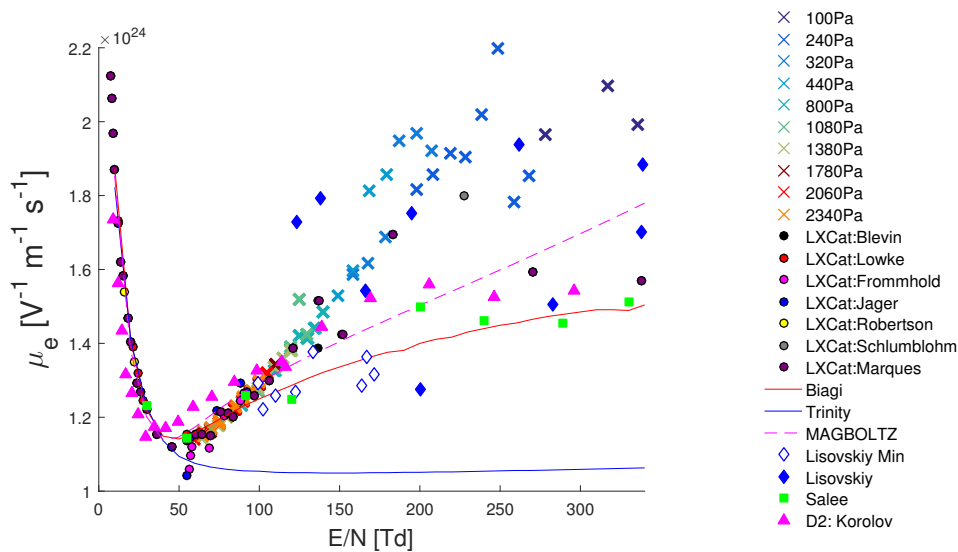


**Figure 3.** The electron mobility, defined as  $w_e = \mu_e \cdot E/N$ , is plotted against  $E/N$ , and compared to reference data and Bolsig+ simulations [12, 14, 16, 17, 19]; furthermore data for deuterium [15].

As for the ionization rate coefficient, our values for the electron mobility, figure 3, agree with reference values below 150 Td, and deviate for higher  $E/N$ , where most referenced authors find a lower mobility. It is not unlikely that our values there are fitted too high: at the lower measurement pressures, we are unable to observe the arrival of the electrons directly, due to strong longitudinal diffusion; therefore the fitting is rather indirect.

Figure 4 shows the fitted mobility of the positive ion, which is presumably mainly  $H_3^+$ . Below 100 Td, our measurement is not suitable for deducing this mobility since the ionization is low and the ion signal too weak, resulting in a strong spread. We find lower values than Miller et al [4], Ellis et al [5], and reports from Georgia Tech (1970-74) (the latter two taken from the Viehland database [10] on LXCat [16]) over the whole measurement range.

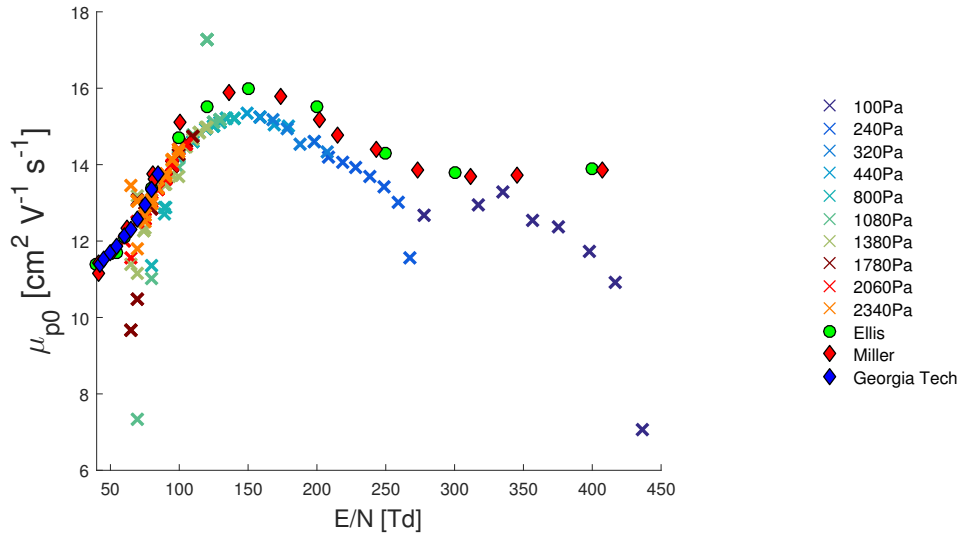


**Figure 4.** The fitted ion mobility for the positive ion is compared to reference data for  $H_3^+$  [4, 5, 16] from LXCat. The mobility is normalized to particle density  $N = 2.686 \cdot 10^{25} \text{ m}^{-3}$  ("standard conditions"), in order to ensure comparability to older literature values. The measurement was done at a temperature of 25°C.

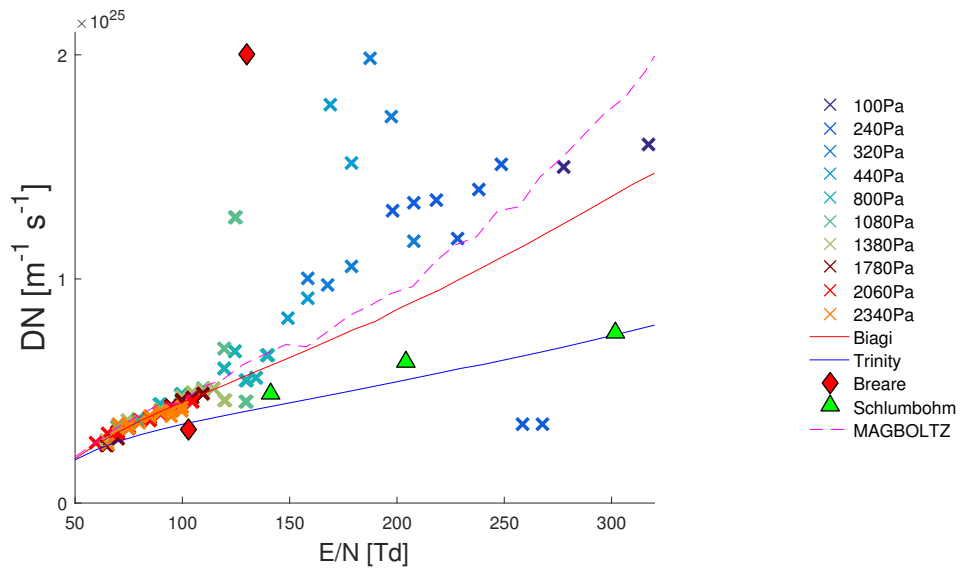


**Figure 5.** The fitted diffusion is compared to reference values of [2, 3] as well as Bolsig+ simulations using Biagi's dataset (MAGBOLTZ version 8.9) [16], TRINITY database [14], and a MAGBOLTZ simulation (version 11.2) [17].

The density-normalized diffusion of hydrogen is shown in figure 5. Our values seem to support the MAGBOLTZ simulation and the Bolsig+ calculations based on Biagi's dataset. Above 150 Td, the quality of the fit degrades strongly.

In order to explain the measured current, a UV light emission rate coefficient was introduced in the model. We fit an (over-)exponential increase (figure 6). Surprisingly, the various excitations of hydrogen (according to Bolsig+ using Biagi's cross sections)

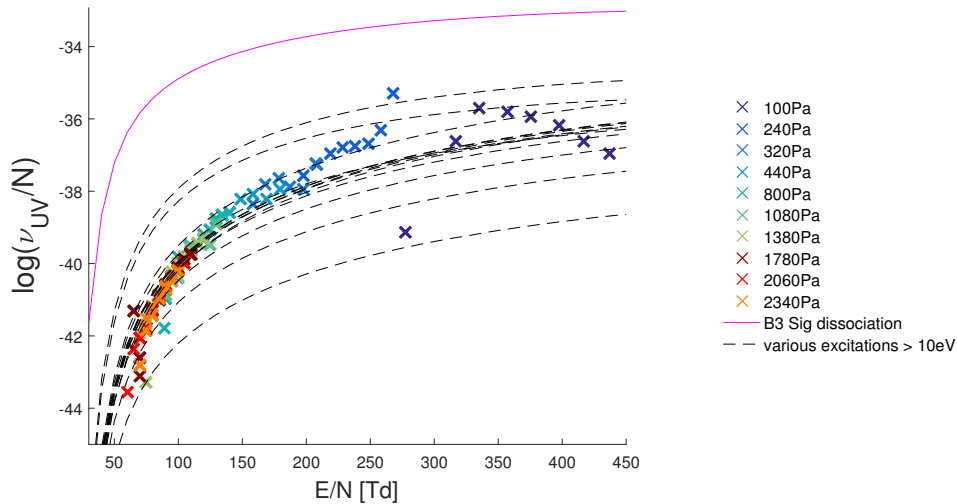


**Figure 6.** The fit for the UV secondary emission shows an exponential increase with increasing  $E/N$ . For comparison, excitation rate coefficients of  $H_2$  are plotted according to a Bolsig+ simulation using Biagi’s database [17].

seem to be of the same magnitude as the fitted UV emission rate. Furthermore, there is no excitation of similar photon energy as the laser which we use for back-illumination, but rather at energies of 8 eV and more.

#### 4. Discussion

Using a simple model for secondary emission, we are able to fit measurements up to 200 Td and recreate the complex waveform of the hydrogen discharge in homogeneous fields for pressures up to 2 kPa. Our results for the swarm parameters fit well to literature, and serve as a check that this model works well. We therefore agree with Phelps [8, 13], and Fletcher and Blevin [6], that photonic secondary electron emission dominates below 200 Td, and present for the first time an evaluation in a Pulsed Townsend experiment of the oscillating current. We are, however, unable to fit the waveforms at higher  $E/N$ .

It is difficult to decide which of the hydrogen’s excitations is responsible for the secondary emission without measuring the emitted spectrum. The supposed UV emission rate implies a very high efficiency of the electron release: Summing up every possible excitation of the Bolsig+ simulation yields a rate that is only a factor of 50 – 100 larger than what is required to explain the measured current. Compared to our usual efficiency of  $10^{-6} - 10^{-8}$  electrons per photon via back-illumination, the rate seems extremely high. Furthermore, the laser is operated at a photon energy of 4.8 eV, for which we try to optimize the cathode; hydrogen, on the other hand, features excitations of sufficient energy only above 8 eV. This suggests that either the lower energy of our laser, or the back-illumination decreases the efficiency substantially.

It seems likely that we did not model the secondary emission by positive ions/neutral



molecules correctly. Two factors might come into play, which are non-trivial to implement: the transversal diffusion, which might be non-negligible in hydrogen at low pressures, could "shift" the ion current radially away from the photo-cathode. This might decrease the strength of the secondary emission over time. Secondly, if Phelps assumption of excitation via neutral hydrogen, which is continuously produced by  $H_3^+$  breakdown, is correct, the model is probably too simple. Instead of releasing an electron with a certain probability per arriving positive ion, the hydrogen radicals should be simulated.

## References

- [1] PH Dawson and AW Tickner. "Detection of  $H_3^+$  in the hydrogen glow discharge". In: *The Journal of Chemical Physics* 37.3 (1962), pp. 672–673.
- [2] JM Breare and A Von Engel. "Locating electron swarms in hydrogen by far ultraviolet signals". In: *Proceedings of the Royal Society of London A: Mathematical, Physical and Engineering Sciences*. Vol. 282. 1390. The Royal Society. 1964, pp. 390–402.
- [3] H Schlumbohm. "Messung der Driftgeschwindigkeiten von Elektronen und positiven Ionen in Gasen". In: *Zeitschrift für Physik A Hadrons and Nuclei* 182.3 (1965), pp. 317–327.
- [4] TM Miller et al. "Reactions of  $H^+$  in  $H_2$  and  $D^+$  in  $D_2$ ; Mobilities of Hydrogen and Alkali Ions in  $H_2$  and  $D_2$  Gases". In: *Physical Review* 173.1 (1968), p. 115.
- [5] HW Ellis et al. "Transport properties of gaseous ions over a wide energy range". In: *Atomic Data and Nuclear Data Tables* 17.3 (1976), pp. 177–210.
- [6] J Fletcher and HA Blevin. "The nature of the positive ion contribution to a gas discharge". In: *Journal of Physics D: Applied Physics* 14.1 (1981), p. 27.
- [7] MS Huq, LD Doverspike, and RL Champion. "Electron detachment for collisions of  $H^-$  and  $D^-$  with hydrogen molecules". In: *Physical Review A* 27.6 (1983), p. 2831.
- [8] AV Phelps, Z Petrović, and BM Jelenković. "Oscillations of low-current electrical discharges between parallel-plane electrodes. III. Models". In: *Physical Review E* 47.4 (1993), p. 2825.
- [9] PM Dehmer and WA Chupka. "Rydberg state reactions of atomic and molecular hydrogen". In: *The Journal of Physical Chemistry* 99.6 (1995), pp. 1686–1699.
- [10] LA Viehland and CC Kirkpatrick. "Relating ion/neutral reaction rate coefficients and cross-sections by accessing a database for ion transport properties". In: *International journal of mass spectrometry and ion processes* 149 (1995), pp. 555–571.
- [11] I Stefanović and ZL Petrović. "Volt Ampere Characteristics of Low Current DC Discharges in Ar, H<sub>2</sub>, CH<sub>4</sub> and SF<sub>6</sub>". In: *Japanese journal of applied physics* 36.7S (1997), p. 4728.

- [12] V Lisovski et al. “Electron drift velocity in argon, nitrogen, hydrogen, oxygen and ammonia in strong electric fields determined from rf breakdown curves”. In: *Journal of Physics D: Applied Physics* 39.4 (2006), p. 660.
- [13] AV Phelps. “Energetic ion, atom, and molecule reactions and excitation in low-current  $H_2$  discharges: model”. In: *Physical Review E* 79.6 (2009), p. 066401.
- [14] NA Dyatko et al. *EEDF: the software package for calculations of the electron energy distribution function in gas mixtures*. 2011.
- [15] I Korolov, M Vass, and Z Donkó. “Scanning drift tube measurements of electron transport parameters in different gases: argon, synthetic air, methane and deuterium”. In: *Journal of Physics D: Applied Physics* 49.41 (2016), p. 415203.
- [16] LC Pitchford et al. “LXCat: an Open-Access, Web-Based Platform for Data Needed for Modeling Low Temperature Plasmas. Date of retrieval: 27.04.2017”. In: *Plasma Processes and Polymers* (2016). DOI: [10.1002/ppap.201600098](https://doi.org/10.1002/ppap.201600098).
- [17] SF Biagi. “MAGBOLTZ, program to compute gas transport parameters”. In: *Version 11.2* (2017).
- [18] A Hösl, P Haefliger, and CM Franck. “Measurement of ionization, attachment, detachment and charge transfer rate coefficients in dry air around the critical electric field”. In: *Journal of Physics D: Applied Physics* 50.48 (2017), p. 485207.
- [19] HT Saelee. *PhD Thesis 1976, University of Liverpool*.